

MINIMIZATION OF SURFACE DEFECTS BY INCREASING THE SURFACE TEMPERATURE DURING THE STRAIGHTENING OF A CONTINUOUSLY CAST SLAB

ZMANJŠEVANJE POVRŠINSKIH NAPAK Z ZVIŠANJEM TEMPERATURE POVRŠINE KONTINUIRNO ULITEGA SLABA MED RAVNANJEM

Josef Stetina, Tomáš Mauder, Lubomir Klimes, Frantisek Kavicka

Brno University of Technology, Technická 2, 616 69 Brno, Czech Republic
stetina@fme.vutbr.cz

Prejem rokopisa – received: 2012-08-31; sprejem za objavo – accepted for publication: 2012-10-23

Surface temperatures of cast slabs on small-radius segments as well as on the unbent areas belong to the parameters that affect the surface quality of continuously cast slabs. Older machines for continuous casting were designed with regard to the quantity (the amount of cast slabs) rather than the quality of the production. Therefore, an adaptation of the secondary cooling is required in order to obtain the desired surface temperatures. The modification consists of a dynamic control of the secondary cooling, surface-temperature monitoring by means of a numerical model of the temperature field as well as a prospective replacement of the cooling nozzles. In order to optimize and control the secondary cooling, characteristics of the nozzles, especially the influences of the water-flow rate, air pressure, casting speed, surface temperatures and heat-transfer coefficient under the nozzles have to be known. Moreover, the heat-transfer coefficient can also be influenced by the age of the nozzles. The paper deals with the relationships between these influences and their impacts on the temperature field of a cast slab. The results are presented for the 1530 mm × 250 mm slabs that are cast in Evraz Vítkovice Steel where the main author's dynamic, 3D solidification model is used, in its off-line version, to control the production interface. The results can be used for the preparation of a real casting process.

Keywords: optimization of the temperature field, surface temperature of a slab, characteristics of nozzles, continuous casting

Temperatura površine ulitega slaba pri segmentih z majhnim radiusom, kot tudi na neukrivljeni površini, spada k parametrom, ki vplivajo na kvaliteto površine kontinuirno ulitega slaba. Starejše naprave za kontinuirno ulivanje slabov so bile pripravljene bolj za večjo zmogljivost kot pa za kvaliteto. Zato je potrebna prilagoditev sekundarnega ohlajanja, da se zagotovi doseganje želene temperature površine. Prilagoditev sestoji iz dinamične kontrole sekundarnega hlajenja, kontrole temperature površine z numeričnim modelom temperaturnega polja, kot tudi morebitna zamenjava hladilnih šob. Optimiranje in kontrola sekundarnega hlajenja je mogoča s poznanjem značilnosti šob in še posebno vpliva hitrosti pretoka vode, tlaka zraka, hitrosti ulivanja, temperature površine in koeficienta prenosa toplote pod šobami. Poleg tega na koeficient prenosa toplote lahko vpliva tudi starost šob. Ta članek obravnava odnos med naštetimi vplivi in njihov učinek na temperaturno polje ulitega slaba. Predstavljeni so rezultati za ulit slab 1530 mm × 250 mm. Avtorjev dinamični 3D-model strjevanja se uporablja za kontrolo vmesnika pri proizvodnji in teče v off-line-verziji. Rezultati se lahko uporabijo kot pripravljalno orodje za realni postopek ulivanja.

Ključne besede: optimiranje temperaturnega polja, temperatura površine slaba, značilnosti šob, kontinuirno ulivanje

1 INTRODUCTION

The presented in-house model of the transient-temperature field of the blank from a slab caster (**Figure 1**) is unique as, in addition to being entirely 3D, it can work in real time. The numerical model covers the temperature field of the complete length of the blank (i.e., from the meniscus inside the mould all the way down to the cutting torch) with up to one million nodes.¹

The concasting machine (caster) for the casting of slabs (**Figure 1**) has the secondary-cooling zone subdivided into thirteen sections due to the convection of a greater amount of heat from the voluminous slab casting. The first section engages the water nozzles from all sides of a slab. The remaining twelve sections engage air-mist cooling nozzles, positioned only on the upper and lower sides of the concasting. It is therefore very important to determine the correct boundary conditions for a numeri-

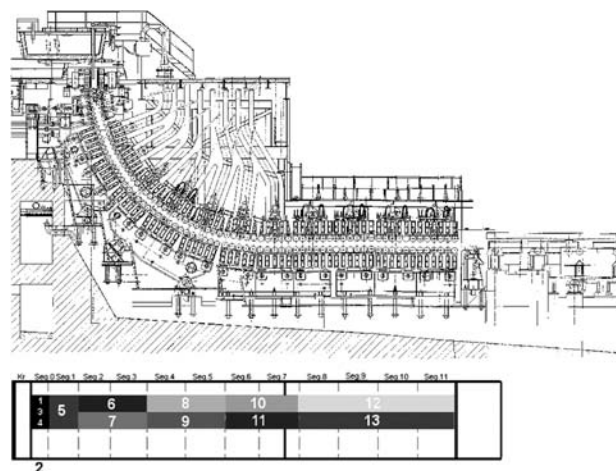


Figure 1: Radial caster and positions of the nozzles along the slab caster in 13 individual zones

Slika 1: Livni stroj z radijem in pozicija šob vzdolž naprave za ulivanje slabov v 13 posameznih področjih

cal model of the temperature field² taking into account a real caster that has many types of nozzles with various settings positioned inside a closed cage. A real caster contains a total of 8 nozzle types and geometrical layouts. The aim is to modify the secondary cooling zones 6, 8, and 10 so as to increase the surface temperature of a slab in a small radius at the point of the straightening. Currently, the Lechler 100.638.30.24 air-mist nozzles are installed in the cooling zones 6, 8, and 10 (Figure 2).

2 MODEL OF THE TEMPERATURE FIELD OF A SLAB

The presented in-house model of the transient-temperature field of the blank from a slab caster (Figure 1) is unique as, in addition to being entirely 3D, it can work in real time. It is possible to adapt its universal code and apply it to any slab caster. The numerical model covers the temperature field of the complete length of the blank (i.e., from the meniscus inside the mould all the way down to the cutting torch) with up to one million nodes.

The temperature field of the slab passing through a radial caster with a large radius can be simplified with the Fourier-Kirchhoff equation, where only the v_z component of the velocity is considered.

$$\rho \cdot c \frac{\partial T}{\partial \tau} = \frac{\partial}{\partial x} \left(k \frac{\partial T}{\partial x} \right) + \frac{\partial}{\partial y} \left(k \frac{\partial T}{\partial y} \right) + \frac{\partial}{\partial z} \left(k \frac{\partial T}{\partial z} \right) + \rho \cdot c \cdot v_z \frac{\partial T}{\partial z} + \dot{Q}_{\text{source}} \quad (1)$$

Equation (1) must cover the temperature field of the blank in all three stages: above the liquidus temperature (i.e., the melt), the interval between the liquidus and solidus temperatures (i.e., the so-called mushy zone) and beneath the solidus temperature (i.e., the solid phase). It is therefore convenient to introduce the thermodynamic

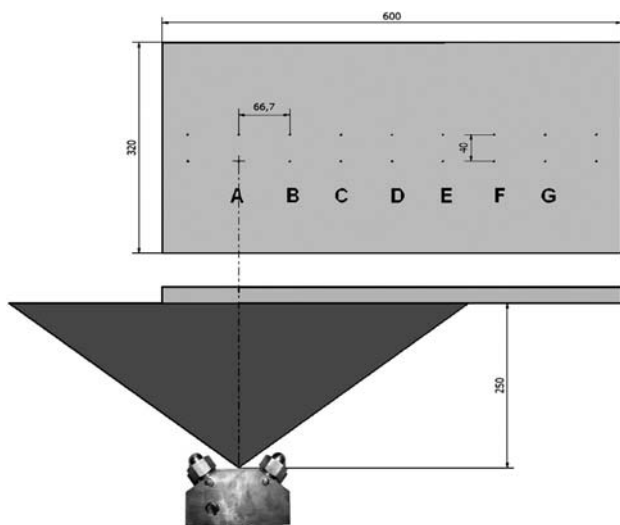


Figure 2: Diagram of the measurement configuration of the cooling effects of a nozzle

Slika 2: Prikaz konfiguracije meritve hladilnih učinkov šobe

function of specific volume enthalpy $H_v = c\rho T$, which is dependent on the temperature and also includes the phase and structural heats (Figure 3).

Heat conductivity k , specific heat capacity c and density ρ are thermophysical properties that are also the functions of temperature. Equation (1) therefore takes the following form:

$$\frac{\partial H_v}{\partial \tau} = \frac{\partial}{\partial x} \left(k \frac{\partial T}{\partial x} \right) + \frac{\partial}{\partial y} \left(k \frac{\partial T}{\partial y} \right) + \frac{\partial}{\partial z} \left(k \frac{\partial T}{\partial z} \right) + v_z \frac{\partial H_v}{\partial z} \quad (2)$$

The unknown enthalpy of the general node of the blank in the following instant ($\tau + \Delta\tau$) is given by the explicit formula:

$$H_{vi,j,k}^{(\tau+\Delta\tau)} = H_{vi,j,k}^{(\tau)} + (QZ1_{i,j} + QZ_{i,j} + QY1_{i,j} + QY_{i,j} + QX1 + QX) \cdot \frac{\Delta\tau}{\Delta x \cdot \Delta y \cdot \Delta z} \quad (3)$$

Figure 3 indicates how the temperature model for the calculated enthalpy in equation (3) determines the unknown temperature³. All the thermodynamic properties of cast steel, dependent on its chemical composition and the cooling rate, enter the calculation as the functions of temperature.³ This is therefore a significantly non-linear task because, even with the boundary conditions, their dependence on the surface temperature of the blank is considered here.

The boundary conditions are, therefore, as follows:

1. $T = T_{\text{cast}}$ the level of steel (4a)
2. $-k \frac{\partial T}{\partial n} = 0$ the plane of symmetry (4b)
3. $-k \frac{\partial T}{\partial n} = htc \cdot (T_{\text{surface}} - T_{\text{mould}})$ inside the mould (4c)

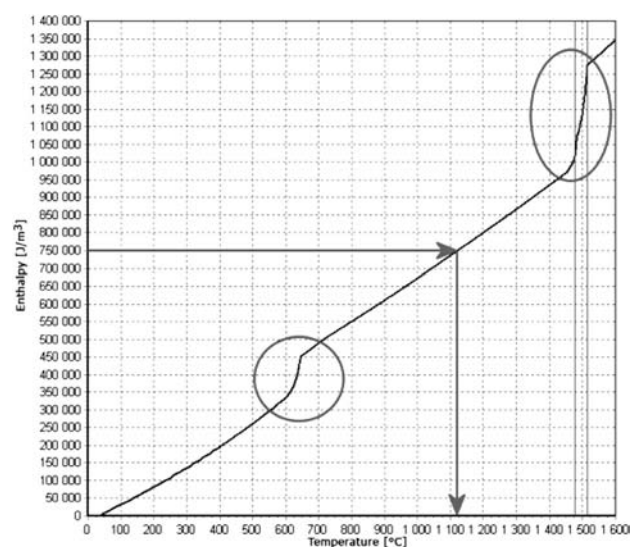


Figure 3: Enthalpy function for steel showing the phase and structural changes

Slika 3: Krivulja entalpije jekla, ki prikazuje fazne preme in spremembe v mikrostrukturi

$$4. -k \frac{\partial T}{\partial n} = htc \cdot (T_{\text{surface}} - T_{\text{amb}}) + \sigma \epsilon (T_{\text{surface}}^4 - T_{\text{amb}}^4)$$

within the secondary and tertiary zones (4d)

$$5. -k \frac{\partial T}{\partial z} = \dot{q} \text{ beneath the rollers} \quad (4e)$$

The boundary conditions are divided into the area of the mould, the area of the secondary cooling and the area of the tertiary cooling.

The initial condition for the investigation is the setting of the temperature in individual points of the mesh. A suitable temperature is the highest possible temperature, i.e., the pouring temperature. The explicit difference method is used for solving this problem. The characteristic of this method is that the stability of the calculation is dependent on the magnitude of the time step. The model uses a method for adapting the time step, i.e., the time step entered by an operator is merely a recommendation and the software is modifying it throughout the calculation.⁴

3 HEAT-TRANSFER COEFFICIENT OF THE NOZZLE

The cooling by the air-mist water nozzles has the main influence and it is, therefore, necessary to establish the relevant heat-transfer coefficient of the forced convection. Commercially sold models of the temperature field describe the heat-transfer coefficient beneath the nozzles as a function of the incident quantity of water per unit area. They are based on various empirical relationships. However, this procedure is undesirable. The model discussed in this paper obtains its heat-transfer coefficients from the measurements of the spraying characteristics of all the nozzles used by the caster on the so-called hot plate in an experimental laboratory and for a sufficient range of operational pressures of water and a sufficient range of casting speeds of a slab. This

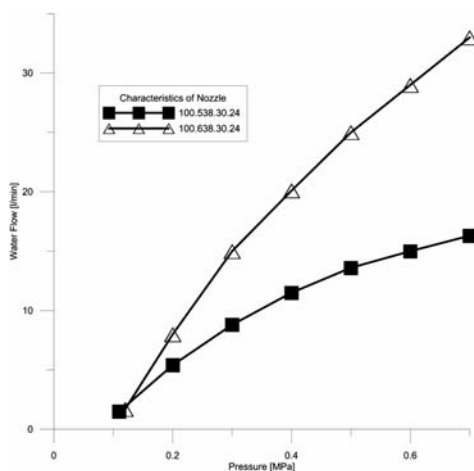


Figure 4: Characteristics of the Lechler nozzles 100.638.30.24 and 100.528.30.24

Slika 4: Značilnosti šobe Lechler 100.638.30.24 in 100.528.30.24

approach represents a unique combination of an experimental measurement in a laboratory and a numerical model for the calculation of the non-linear boundary conditions beneath the cooling nozzle.

A laboratory device enables separate measurements of individual nozzles. It includes a steel plate mounted with 18 thermocouples, heated by an external electric source. The steel plate is heated to the testing temperature, than it is cooled by a cooling nozzle. On the return move the nozzle is covered with a deflector, which enables the movement of the nozzle without cooling the surface. This device measures the temperatures beneath the surface of the slab – again by means of thermocouples.⁵

The laboratory device allows the setting of:

- the nozzle type,
- the flow of water,
- the air pressure,
- the distance between the nozzle and the investigated surface,
- the surface temperature,
- the shift rate.

Since the cooling nozzle 100.638.30.24 for the minimum water flow appeared to be too intense, the measurements were made for the smaller nozzle 100.528.30.24 (Figure 4).

Based on the temperatures measured in dependence of the time, the heat-transfer coefficients (*htc*) are calculated with an inverse task. They are then processed further using an expanded numerical and identification model and converted to the coefficients of function *htc(T,y,z)* (Figure 5), which express *htc* in dependence of the surface temperature and also the position of the con-casting with respect to the nozzle. The Lechler air-mist nozzles show a low dependence of the heat-transfer coefficient on the slab surface temperature. The value of *htc* on the surface of a slab, as it enters the secondary-cooling zone, significantly affects the process simulation with respect to the temperature field, the metallurgical length and also the other technological properties. It, therefore, affects the prediction of the quality of a slab.

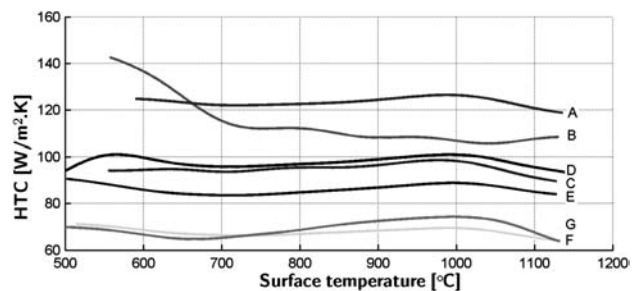


Figure 5: Heat-transfer coefficient as a function of the surface temperature

Slika 5: Koefficient prenosa toplote v odvisnosti od temperature površine

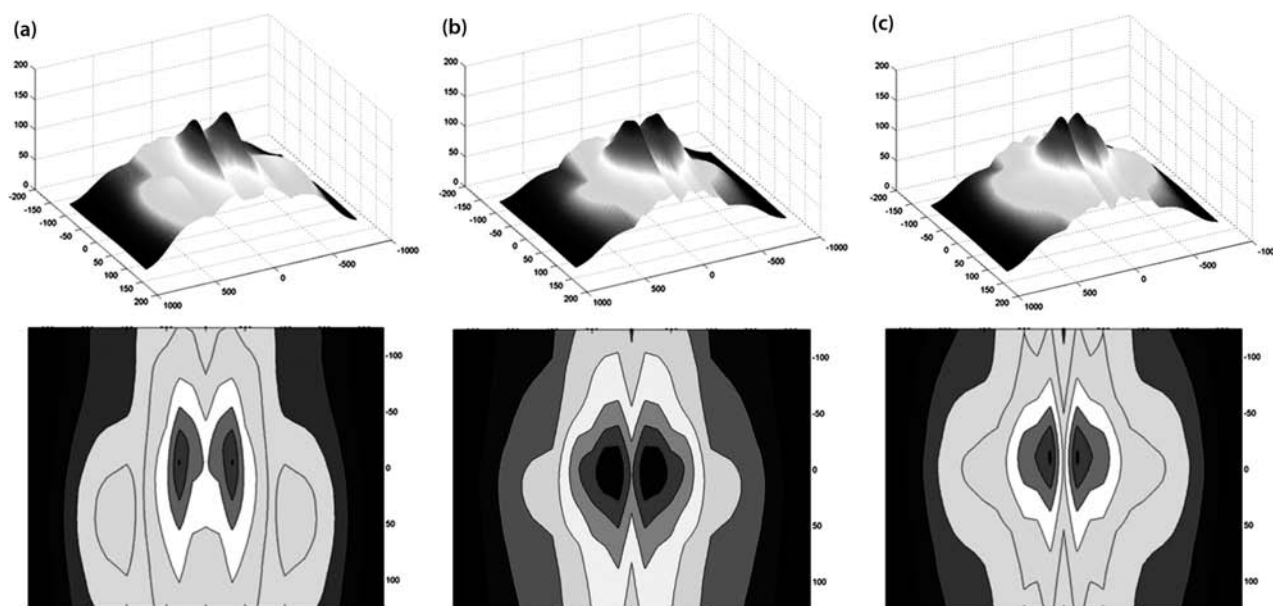


Figure 6: Heat-transfer coefficient for the Lechler air-mist nozzle: a) nozzle 100.638.30.24 with the water flow of 2.2 L/min and air pressure of 0.2 MPa, b) nozzle 100.528.30.24 with the water flow of 2.2 L/min and air pressure of 0.2 MPa, c) nozzle 100.528.30.24 with the water flow of 1.5 L/min and air pressure of 0.2 MPa

Slika 6: Koeficient prenosa toplote pri Lechler šobi za ustvarjanje zračne megle: a) šoba 100.638.30.24, pretok vode 2,2 L/min, zračni tlak 0,2 MPa, b) šoba 100.528.30.24, pretok vode 2,2 L/min, zračni tlak 0,2 MPa, c) šoba 100.528.30.24, pretok vode 1,5 L/min, zračni tlak 0,2 MPa

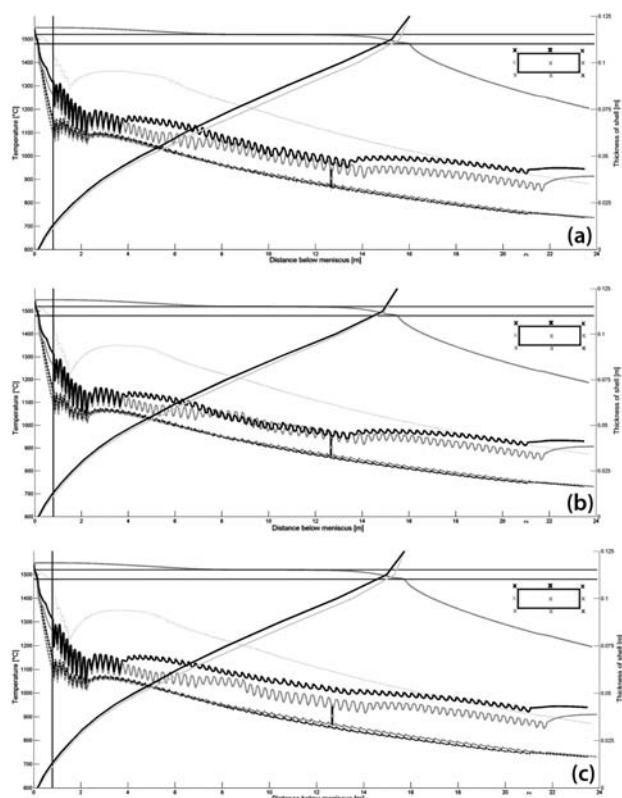


Figure 7: Temperature history along the caster for different configurations of secondary cooling in zones 6, 8 and 10: a) nozzle 100.638.30.24 with the water flow of 2.2 L/min per nozzle, b) nozzle 100.528.30.24 with the water flow of 2.2 L/min per nozzle, c) nozzle 100.528.30.24 with the water flow of 1.5 L/min and air pressure of 0.2 MPa

Slika 7: Zgodovina temperature vzdolž livne naprave za različno izvedbo sekundarnega hlajenja v conah 6, 8 in 10: a) šoba 100.638.30.24, pretok vode skozi šobo 2,2 L/min, b) šoba 100.528.30.24, pretok vode skozi šobo 2,2 L/min, c) šoba 100.528.30.24, pretok vode 1,5 L/min, zračni tlak 0,2 MPa

In order to be able to simulate this boundary condition within the numerical model as accurately as possible, it is necessary to conduct an experimental measurement on each nozzle in the secondary-cooling zone.

Each of the eight nozzles was measured separately with the hot model, on which the hot surface of the slab, cooled by a moving nozzle, can be modelled. The temperatures measured on the surface of the model can be entered into an inverse task to calculate the intensity of spraying, which, in turn, can determine *htc* with a special mathematical method.

Figure 5 presents the measured values of the heat-transfer coefficients processed by the temperature model software. For the nozzle configuration, there is a graph of the 3D graph (**Figure 6**) of the heat-transfer coefficient beneath the nozzle. These graphs are plotted for surface temperatures from 800 °C to 1000 °C.

4 TEMPERATURE FIELD

The setting of the secondary cooling and its optimization is a very complicated problem. The graph in **Figure 7** shows the resultant temperature fields for individual cooling curves. This basic set of graphs serves the user making it possible to assess which of the cooling

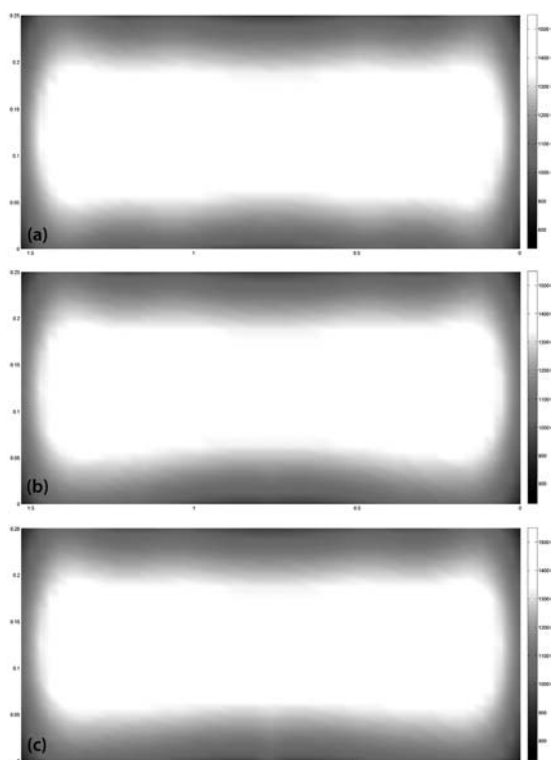


Figure 8: Temperature field at the cross-section of the slab at the straightening point:

- a) nozzle 100.638.30.24 with the water flow of 2.2 L/min per nozzle,
- b) nozzle 100.528.30.24 with the water flow of 2.2 L/min,
- c) nozzle 100.528.30.24 with the water flow of 1.5 L/min

Slika 8: Temperaturno polje na prerezu slaba v točki ravnjanja:

- a) šoba 100.638.30.24, pretok vode skozi šobo 2,2 L/min,
- b) šoba 100.528.30.24, pretok vode skozi šobo 2,2 L/min,
- c) šoba 100.528.30.24, pretok vode skozi šobo 1,5 L/min

curves is optimal for the given cast steel³. **Figure 7a** shows the surface temperature of the slab in the caster using nozzle 100.638.30.24 with the secondary-cooling flow of 2.2 L/min per nozzle. **Figure 7b** shows the temperature for the same conditions, but only for zones 6, 8, and 10 using nozzle 100.528.30.24. **Figure 7c** shows the surface temperature for the water flow of 1.5 L/min for nozzle 100.528.30.24 in zones 6, 8, and 10. These calculations show that the new nozzles increase the surface temperature at the straightening point of a small radius by about 100 °C, while with the higher water-flow rates a new nozzle can cool as intensely as the original nozzle. **Figure 8** shows the temperature field in the cross-section at the straightening point using the same parameters as for **Figure 7**.

The increase in the surface temperature in the straightening point on the small-radius surface has definitely helped to reduce the surface defects of cast slabs. This conclusion is also confirmed by the macrostructure figures that were made for two slabs of 1530 mm × 250 mm and a steel grade S275. **Figure 9a** shows the macrostructure of the steel that was cast with the previous setup of the cooling (the Lechler nozzle 100.638.30.24 with the flow rate of 2.2 L/min) and

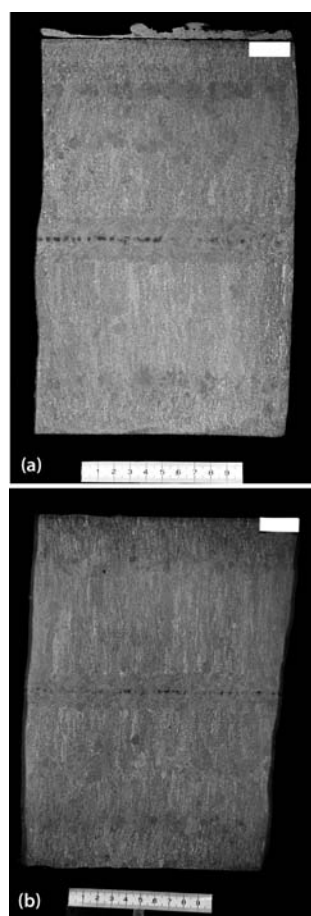


Figure 9: Macrostructure of the slab before and after the adjustment of the secondary cooling of steel S 275:

- a) nozzle 100.638.30.24 with the water flow of 2.2 L/min per nozzle,
- b) nozzle 100.528.30.24 with the water flow of 1.5 L/min per nozzle

Slika 9: Makrostruktura plošče pred prilagoditvijo sekundarnega hlajenja jekla S 275 in po njej:

- a) šoba 100.638.30.24, pretok vode skozi šobo 2,2 L/min,
- b) šoba 100.528.30.24, pretok vode skozi šobo 1,5 L/min

Figure 9b presents the macrostructure obtained with the use of the new setup of the cooling (the Lechler nozzle 100.528.30.24 with the flow rate of 1.5 L/min). The new setup of the cooling has been used on the caster since July 2012, and therefore the statistical evaluation of the surface defects from the operational data is not yet available.

5 CONCLUSIONS

It has been proved that the value of the heat-transfer coefficient on the surface of the slab and the heat withdrawal in the secondary-cooling zone significantly affect the process simulation from the viewpoint of the temperature field, the metallurgical length and also the other technological properties. Moreover, these parameters also influence the surface quality of cast slabs and therefore they enable us to predict the quality of the slabs. In order to simulate the boundary condition of the numerical model as accurately as possible, it is necessary

to conduct experimental measurements for each nozzle in the secondary cooling zone. For this purpose, all the used nozzles were measured separately with the hot model, with which the hot surface of the slab, cooled by a moving nozzle, can be modelled.

The original 3D numerical model of the temperature field was used for optimizing the surface temperatures of cast slabs⁶. The results are presented for the 1530 mm × 250 mm slabs that are cast in Evraz Vitkovice Steel, Czech Republic. The performed optimization proved that a proper replacement of the cooling nozzles in the secondary cooling zone and a reduction of the flow rate through the nozzles can help to increase the surface temperature of a cast slab in the straightening point so that the surface defects can be reduced. Besides, it was also shown, for a particular pair of the Lechler nozzles, that although a nozzle is replaced with a smaller one, in the cases of higher flow rates, it can have the same cooling intensity as a larger nozzle.

Acknowledgments

The authors gratefully acknowledge the financial support from the project GACR P107/11/1566 founded by the Czech Science Foundation, project ED0002/01/01 of the NETME Centre, and Specific Research FSI-J-12-22. The co-author, the recipient of the Brno PhD Talent Financial Aid sponsored by the Brno City Municipality, also gratefully acknowledges the financial support.

Nomenclature

c	specific heat capacity	J/kg K
htc	heat transfer coefficient	W/(m ² K)
H_v	volume enthalpy	J/m ³

k	heat conductivity	W/(m K)
T	temperature	K
T_{amb}	ambient temperature	K
T_{cast}	melt temperature	K
$T_{surface}$	temperature in unbending part	K
\dot{q}	specific heat flow	W/m ²
Q_X, Q_Y, Q_Z	heat flows	W
\dot{Q}_{source}	internal heat source	W/m ³
x, y, z	axes in given direction	m
v_z	casting speed in given direction	m/s
ρ	density	kg/m ³
σ	Stefan-Boltzmann constant	W/m ² K ⁴
ε	emissivity	–
τ	time	s

6 REFERENCES

- ¹ J. P. Birat, The Making, Shaping and Treating of Steel, Casting Volume, 11th edition, Alan W. Cramb (ed.), The AISE Steel Foundation, Pittsburgh, PA, USA, 2003
- ² T. Mauder, J. Stetina, C. Sandera, F. Kavicka, M. Masarik, An optimal relationship between casting speed and heat transfer coefficients for continuous casting process, In Metal 2011, Conference proceedings, Metal. Ostrava, Tanger, 2011, 22–27
- ³ P. Charvat, T. Mauder, M. Ostry, Simulation of latent-heat thermal storage integrated with room structures, Mater. Technol., 46 (2012) 3, 239–242
- ⁴ R. Pyszko, M. Prihoda, P. Fojtik, M. Kovac, Determination of heat flux layout in the mould of continuous casting of steel, Metalurgija (Metallurgy), 51 (2012) 2, 149–152
- ⁵ T. Luks, J. Ondrouskova, J. Horsky, Nozzle cooling of hot surfaces with various orientations, In Experimental fluid Mechanics 2011, Proceedings of the International conference, Jicín, 2011, 337–346
- ⁶ L. Klimes, P. Popela, An Implementation of Progressive Hedging Algorithm for Engineering Problems, In Mendel 2010 – 16th International Conference on Soft Computing, Brno, BUT, 2010, 459–464